2012-05-07

Mechanism of Inhibition of Influenza A Virus M2 Proton Channel

Douglas Randall Bretzing
dougwhit20@gmail.com

Victoria Man-Fung Burr

Mechanism of Inhibition of Influenza A Virus M2 Proton Channel

Douglas Bretzing[*] and Victoria Burr[+]

[*]*Department of Physiology and Developmental Biology, Brigham Young University, Provo, UT 84602, USA.* [+]*Department of Chemistry and Biochemistry, Brigham Young University, Provo, UT 84602, USA.*

April 11, 2012

Abstract

The influenza A virus integral membrane protein, M2, is a proton-conducting channel. The ability of influenza A virus to unpack its genome, replicate, and infect its host is contingent upon the M2-mediated acidification of the viral interior. The antiviral drugs amantadine and rimantadine were previously effective in blocking proton influx through M2; however, mutations in the proton channel have rendered these drugs ineffective. Multiple models for the inhibiting mechanism of the adamantane drugs have been hypothesized. In an attempt to better understand the mechanism of M2 inhibition, and ultimately to assist in the development of a replacement M2-targeting antiviral drug, we have set out to determine the site of interaction between rimantadine and M2 using native chemical ligation, a reaction that will result in the formation of a peptide bond between the cysteine residue of mutated M2 and a rimantadine thiol group. We report that we have made significant progress towards growth, harvest, and purification of the M2 (22-62) mutants S31C and G34C (mutation names being based on the full-length protein residue numbers). Additionally, we have successfully synthesized the second to last intermediate, an azido alcohol, of our rimantadine thiol synthesis scheme with 82% yield. This report indicates our progress towards the completion of our project, a project which we believe will assist with further understanding the interaction between M2 and antiviral drugs.

Introduction

The ability of influenza A virus to unpack its genome, replicate, and infect its host is contingent upon acidification of the viral interior. This is achieved by proton conductance via M2, an integral membrane protein that forms proton channels in the viral lipid envelope of influenza A virus (1). The drugs amantadine and rimantadine have previously been successful in

blocking proton flux into the virus, however viral resistance to these drugs has recently reached over 90% (2.). Early models of the M2 channel protein of influenza A virus propose that the antiviral drugs amantadine and rimantadine interact with pore-lining residues within the channel, thereby blocking proton influx and disabling the virus. Stouffer et al. (2) have supported this hypothesis with their results using x-ray crystallography. They report that crystals grown in the presence of amantadine showed electron-density within the M2 channel of the same size and shape as that of the amantadine molecule, surrounded by pore lining residues whose mutations are generally accepted as being the mechanism for the virus' drug resistance to the adamantane drugs (2).

However, Schnell and Chou have offered a well supported alternative hypothesis. Using NMR to test rimantadine bound M2, they detected drug NOEs at a residue (D44) outside the channel pore at the C terminus of the protein, but were unable to detect drug NOEs anywhere within the pore of the channel (1). Cady et al. (3), using solid state NMR spectroscopy, concluded that both the pore and C terminus of the channel act as amantadine-binding sites. However, they found that amantadine binds to the pore of the channel with much higher affinity than it binds to the C-terminal protein surface (3).

We intend to further investigate the binding site of the adamantane drugs using native chemical ligation. Native chemical ligation is a reaction in which the thiolate group of a cysteine attacks the thioester group of a second molecule (4) (Figure 1). We will use native chemical ligation to form an amide bond between a drug (rather than peptide 2, as shown in Figure 1), namely rimantadine, and modified M2 (22-62) S31C (i.e. the truncated, site-mutated protein; this mutated, truncated protein will be referred to as M2 throughout the remainder of this report, except as noted). Formation of the amide bond will require mutating the M2 amino acid of

interest to cysteine and creating a reactive form of the drug, replacing a hydrogen atom on a rimantadine methyl group with a thiol group. Native chemical ligation will be performed by mixing the two reactants in a phosphate buffer (pH 7.4) at room temperature for one hour (5). We will test the functionality of the M2 mutants, both before and after formation of the rimantadine-M2 amide bond, using the liposome assay as described by Sharma et al. (6). We will use mass spectrometry to confirm formation of the rimantadine-M2 amide bond using the same sample tested in the liposome assay, if possible. Otherwise, we will use mass spectrometry to test a parallel sample. Here we will report our progress on these aims.

Methods

M2 Growth. We performed site directed mutagenesis using a QuickChange Lightning Site-Directed Mutagenesis Kit (Agilent Technologies, La Jolla, CA) to mutate the residues of interest to cysteine. Ian Nelson generously performed the site directed mutagenesis for two mutants, S31C and G34C. The forward sequence of the S31C primer was 5'- GAT TCA AGT GAC CCT CTT GTT GTT GCT GCG **TGT** ATC ATT GGG ATC TTG CAC TTG ATA TTG TGG ATT C -3' (mutated codon in bold). There were 30 base pairs upstream of the mutation, the upstream GC content was 50%, and the T_m upstream of the mutation was 79.5˚ C. There were 34 base pairs downstream of the mutation, the downstream GC content was 38%, and the T_m downstream of the mutation was 78.74˚ C. The forward sequence of the G34C primer was 5'- GAC CCT CTT GTT GTT GCT GCG AGT ATC ATT **TGC** ATC TTG CAC TTG ATA TTG TGG ATT CTT GAT CGT CTT TTT TTC-3' (mutated codon in bold). There were 30 base pairs upstream of the mutation, the upstream GC content was 46.67%, and the T_m upstream of the mutation was 78.27˚ C. There were 42 base pairs downstream of the mutation, the

downstream GC content was 33.33%, and the T_m downstream of the mutation was 78.958˚ C. This report focuses on the effort to grow, purify, and reconstitute the S31C variant.

Following the site directed mutagenesis, *E. Coli* was transfected with each plasmid. LB broth (2 g LB Mix, 0.5 g NaCl, 100 ml ddH_2O) was autoclaved and allowed to cool, after which Ampicillin was added to a final concentration of 50 µg/ml. Approximately 10 µl of bacterial stock was used to inoculate the 10 ml of broth, and the inoculated "starter" broth was incubated at 37˚ C and 220 RPM for 8-12 hours. The optical density at 600 nm was then measured to confirm proper bacterial growth (target optical density was 0.5-1.2), and the contents of the "starter" broth were joined with the remaining 90 ml of autoclaved LB broth. The broth was then incubated at 25˚ C and 220 RPM for 10-16 hours, after which the optical density at 600 nm was again measured (target optical density was 0.5-0.7). M2 growth was induced by addition of IPTG to the broth at a final concentration of 1.0 mM, and the sample was incubated at 16˚ C, while rotating at 220 RPM, for 23-24 hours. The optical density at 600 nm was measured, and the sample was placed on ice for 30 minutes to stop cell growth and prevent proteolysis. The 100 ml of bacterial sample was partitioned into two 50 ml conical base tubes and centrifuged at 4˚ C and 5000 RPM for 30 minutes. The supernatant was discarded and the pellets were re-suspended using 4 ml total of lysis buffer [50 mM Tris-HCl (pH 8.0), 300 mM NaCl, 10 mM Imidazole].

M2 Harvest. The re-suspended pellets were combined in a 15 ml conical base tube and were lysed using a tip sonicator for 60 seconds (1.0 second pulse, 0.2 second pause, 20-30% intensity). The lysed sample was centrifuged at 4˚ C and 7500 RPM for 30 minutes and the supernatant, expected to contain the MBP-containing protein, was carefully collected in a new 15 ml conical base tube (pellet was discarded). Octyl glucoside (O.G.) was added to the supernatant

at a final concentration of 75 mM and the sample was incubated on a shaker at 4˚ C for 4 hours. The sample was then centrifuged at 4˚ C and 7500 RPM for 30 minutes, and the supernatant was carefully poured into a prepared nickel column.

M2 Purification. The nickel column was prepared by adding 0.5-1.0 ml of Ni-NTA (Qiagen GmbH, Hilden, Germany) to a 5 ml disposable column. Ni-NTA was equilibrated by running 10 ml of wash buffer #1 [50 mM Tris-HCl (pH 8.0), 300 mM NaCl, 10 mM imidazole, 5 mM O.G.] through the nickel resin. After addition of the supernatant, the column was incubated on a shaker at 4˚ C for 4 hours in order to facilitate binding of M2 to the Ni-NTA. The column run-through was collected and the column was washed with 20 ml of wash buffer #2 [50 mM Tris-HCl (pH 8.0), 300 mM NaCl, 25 mM imidazole, 5 mM O.G.]. The bound M2 was then carefully eluted from the column using 0.5-1.0 ml (depending on the volume of Ni-NTA used) of elution buffer [50 mM Tris-HCl (pH 8.0), 300 mM NaCl, 250 mM imidazole, 5 mM O.G.]. Fractions of eluted M2 were collected in increments of about 0.1 ml each, and the concentration of protein in each fraction was determined using a spectrophotometer (NanoDrop Technologies, Inc., Wilmington, DE).

Characterization of the contents of each fraction was carried out using Tris-Hepes-SDS gel electrophoresis. 25 μL of each fraction was prepared for electrophoresis using 25 μL of SDS sample loading buffer (4 ml of 10% SDS, 2ml glycerol, 1 ml 0.1% bromophenol blue, 2.5 ml 0.5 M Tris-HCl pH 6.8, deionized water to 10 ml). Tris-HEPES-SDS running buffer (10X) (121 g Tris Base, 238 g HEPES, 10 g SDS, ultrapure water to 1,000 ml) was prepared and diluted 10-fold with ultrapure water. The 1X running buffer (confirmed to be pH 8 without pH adjustment) was used for electrophoresis.

On-Column TEV Cleavage of Ni-NTA-bound M2. M2 was bound to the Ni-NTA, and the column was washed, as described above. Rather than eluting the column, His-tagged TEV protease was added to the column in 4 ml of buffer solution (1X ProTEV Buffer, 1 mM DTT, 400 units ProTEV Plus) and the column was incubated on a shaker at 4˚ C for 20 hours. The column run-through was collected and the presence of cleaved M2-MBP was evaluated using Tris-Hepes-SDS gel electrophoresis.

TEV Protease Cleavage of Column-eluted M2 and Ultrafiltrate Centrifugation. As an alternative to on-column cleavage, eluted protein was cleaved off the column. The Ni-NTA column was eluted as explained in *M2 Purification* above, and the elution fractions containing M2 were combined in a 10 ml beaker. TEV protease was added to the column in 4 ml of buffer solution [1X ProTEV Buffer, 1 mM DTT, 400 units ProTEV Plus (Promega Corporation, Madison, WI)] and the column was incubated on a shaker at room temperature (approximately 21˚ C) for 20 hours. The reaction contents were then incubated in a newly prepared column, as described above. The His-tagged TEV Protease and the cleaved His-tagged MBP from the MBP-M2 protein were expected to bind to the column. The column run-through was collected and assessed for M2-MBP content using Tris-Hepes-SDS gel electrophoresis. The remaining sample was poured into a 3 kD molecular weight cut-off spin filter (Millipore Corporation, Billerica, MA) and spun at 4000 x g for 22 minutes, leaving an unfiltered residue of buffer and M2-MBP. The filtrate was discarded and approximately 3.9 ml of methanol was added to the unfiltered residue sample, bringing the total volume back up to approximately 4.0 ml. This process was repeated 3-4 times, resulting in complete transfer of M2 from elution buffer to methanol. The approximate concentration of the M2 in methanol was determined using the

absorbance of the sample at 280 nm, measured using a Spectronic Genesys 5 UV Spectrophotometer (Thermo, Madison, WI).

M2 Purification Using TCA/methanol Approach. Following TEV cleavage of column-eluted M2 (as described above), the TEV cleavage reaction was stopped by addition of TCA at a final concentration of 6%, resulting in precipitation of all proteins present. The precipitate was collected by centrifuging the sample at room temperature (approximately 21˚ C) and 9000 RPM for 10 minutes. The supernatant was carefully discarded and the pellet was washed with water twice to remove residual TCA. The pellet was vacuumed for 2.5 hours to thoroughly dry the pellet, after which 5 ml of methanol was added to dissolve the M2 in the sample, mixing gently for 4.5 hours at room temperature. The solution was then centrifuged at 13,000 x g for 20 minutes to pellet out insoluble components and the supernatant was carefully collected. The approximate concentration of the M2 in methanol was determined spectroscopically.

Liposome Preparation. Liposomes were prepared by mixing chloroform-suspended 1-palmitoyl 2-oleoylphosphatidylcholine (POPC), 1-palmitoyl 2-oleoylphosphatidylglycerol (POPG), and cholesterol (all used without further purification from Avanti Polar Lipids, Alabaster, AL) at molar proportions of 3:1:2. The solution was vortexed to ensure a homogenous mixture. The solvent was then evaporated off using a steady stream of nitrogen gas. The resulting thin film was vacuumed overnight to ensure the removal of excess solvent. Methanol-suspended M2(22-62) was then added to the lipid thin film, the solution was vortexed, the solvent was evaporated off using a steady stream of nitrogen gas, and the resulting thin film vacuumed for about 1 hour. The thin film was re-suspended in internal buffer (50 mM KCl, 50 mM K_2HPO_4, 50 mM KH_2PO_4, pH 8.0, 320 mOsm) and extruded through a 100-nm pore-size polycarbonate filter at room temperature (approximately 21˚ C). After extrusion, the samples

were divided in two and amantadine was added to one of the samples at a concentration of 0.2 mM and incubated overnight. During the experiment, the amantadine concentration was diluted to 0.1 mM.

Liposome Assay Protocol. A pH electrode (Fisher Scientific, Waltham, MA) was used to measure proton movement into or out of the liposomes throughout the experiment. A pH meter (Cole-Parmer, Vernon Hills, IL) was connected, via its recorder output, to an LPF-8 amplifier (Warner Instruments, Hamden, CT) to obtain a continuous time measurement. The amplifier gain was set at 100 and the lowpass frequency cutoff was set at 20 Hz. LabView 2009 (stripchart code written by Dr. David Busath) was used to collect the data.

30 µL of liposomes were added to 3 ml of citrate external buffer (0.33 mM citric acid, 1.67 mM sodium citrate, 165 mM NaCl, pH 6.4, 310 mOsm) in a 1-dram vial. After one minute, 26 µL of .1 M HCl was added to the solution to reach a desired pH of approximately 6.0. Valinomycin (Sigma-Aldrich Corporation, Saint Louis, MO) was added one minute after HCl addition to a concentration of 30 nM. CCCP was added 2 minutes thereafter to a concentration of 1.67 µM. 30 nEq of HCl was added twice one minute apart, 2 minutes after CCCP addition. Following the presumptive depolarization of the vesicles, buffer effects due to the valinomycin and CCCP solution injections were analyzed by one additional injection each of valinomycin and CCCP. M2 proton conductance was based on the initial flux after valinomycin activation, calibrated with *post hoc* titration tests of the solution's buffer capacity and corrected for the buffer effects by subtraction. The data was analyzed using Microsoft Office Excel 2007 (data analysis program written by Dr. Dixon Woodbury and Emily Peterson).

Rimantadine Thiol Synthesis. Adamantyl bromomethyl ketone (Sigma-Aldrich Corporation, Saint Louis, MO) (1 g, 3.39 mmol) was dissolved in 23 ml of dry methanol. This

solution was brought to 0° C using an ice bath. Two molar equivalents of sodium borohydride ($NaBH_4$) were added in portions. After the addition, the ice bath was removed and the mixture was stirred at room temperature for 1 hour. The reaction was then concentrated *in vacuo* and diluted with water. This aqueous mixture was extracted with Et_2O (3x), washed with NH_4Cl (sat.) and brine, then dried over $NaSO_4$ to give the bromo-alcohol product (945.5 mg, 94% yield). The bromo-alcohol product (945 mg, 3.65 mmol) was treated with 10 ml of 2N NaOH in 20 ml of tetrahydrofuran (THF) for 2 hours at room temperature. We then performed aqueous workup using ether and H_2O, followed by 3 extractions using ether. The combined ether solution was washed with NH_4Cl (sat.) and brine, then dried over $NaSO_4$ to give the epoxide product. Epoxide was purified by flash column chromatography on silica using 5% Ether/Hexanes (618 mg, 95% yield).

The epoxide (618 mg, 3.47 mmol) was dissolved in 17.5 ml of ethanol/H_2O (1:1). Two molar equivalents of NaN_3 and 2 molar equivalents of NH_4Cl were added. This reaction was set to reflux overnight. The reaction was then concentrated *in vacuo*, dissolved in EtOAc, washed with H_2O, dried over $NaSO_4$, and concentrated *in vacuo*. The product was purified *on silica* using 5-10% Ether/Hexanes to give the azido-alcohol product (542.3 mg, 74% yield).

The azido-alcohol (51.4 mg, 0.22 mmol) and 1.1 equivalents of triphenylphosphine (PPh_3) in 3 ml of toluene were heated under reflux overnight. After cooling to room temperature, the mixture was concentrated *in vacuo* and chromatographed using 0-2% MeOH/CH_2Cl_2 to give the aziridine product (13.1 mg, 33% yield).

Report

We were able to achieve a yield of 0.38 ± 0.014 mg of MBP-M2 (as mentioned above, M2 refers to the conductance domain with the S31C mutation) for each 250 ml of bacterial

culture grown. To confirm the identity of the purified protein, we ran our protein sample on a Tris-Hepes-SDS gel. The results of the finished gel were difficult to explain. We show them here as an interim report. The plasmid we used to transfect the *E. Coli* included the DNA corresponding to the mutated M2, preceded by a TEV protease cleavable maltose binding protein (MBP). Each M2 monomer is approximately 5 kD and MBP is approximately 44.1kD. Because the MBP-M2 monomers are unable to form tetramers before TEV cleavage, due to steric interference from the MBP, we expected a single band corresponding to uncleaved M2 at approximately 49 kD because the TEV cleavage site adds only a modest additional mass. Instead, we observed significant bands at 10 kD, 15 kD, 25 kD, and 60 kD (Figure 2 lanes 6-10). The 10 kD, 15 kD, and 25 kD bands present in lanes 6-10 of Figure 2 could correspond to TEV-cleaved M2 dimers, trimers, and tetramers, respectively, possibly covalently linked by disulfide bonds. The 60 kD (lanes 6-10) band could possibly correspond to uncleaved M2 monomers. However, this explanation requires that the MBP-fusion protein is spontaneously cleaving (without being exposed to TEV protease and without producing a 44 kD band on the gel), which is illogical and therefore requires further investigation.

In our first approach to the TEV cleavage reaction, we incubated the TEV protease with MBP-M2 bound to the resin.(0.5 ml, 22.5 hours at 4˚ C). The column runoff, which was expected to contain the cleaved M2, was collected and run on a Tris-Hepes-SDS gel (data not shown). The only significant band was located at 48 kD, corresponding to the molecular weight of the TEV protease, which was expected to stay bound to the resin because of its His-tag. We suppose that the 0.5 ml of nickel resin probably was overloaded and the Ni sites became saturated, resulting in the excess TEV protease appearing in the runoff. We attribute the minimal M2 in the runoff to the low temperature (4˚ C), which may have reduced enzymatic cleavage. It

is also possible that a fraction of the TEV protease bound to the nickel resin and was unavailable to catalyze cleavage of the MBP-M2 construct.

In our second approach to the TEV cleavage reaction, we: 1. eluted the M2-MBP from the nickel column; 2. incubated the M2-MBP with TEV protease in a beaker at room temperature (approximately 21˚ C) for 20 hours; and 3. incubated the sample with 1 ml of nickel resin for 4 hours at 4˚ C. Following this final incubation, 4. the column runoff was collected, and 5. the column was eluted. Lane 3 of Figure 3, containing the column run-through from step 4 (which was expected to contain cleaved M2 22-62 (S31C)), and lane 1 of Figure 3, containing column elution from step 5 (which was expected to contain MBP and TEV protease), appeared exactly the same as each other on the gel, with bands at 10 kD, 15 kD, 25 kD, 48 kD, 55 kD, and 130 kD. Again, it is possible that the nickel resin was saturated (although the volume of resin used was increased from 0.5 ml to 1 ml), thereby accounting for the possible presence of TEV protease (MW of 48 kD) and MBP (MW of 42.5 kD) in the runoff. The apparent presence of cleaved M2 dimers, trimers, and tetramers (10 kD, 15 kD, and 20 kD, respectively) in the column elution fraction, which should have been free of M2, is likely the result of our inadvertently not washing the column after collecting the runoff.

There are multiple approaches to reconstituting M2 into liposomes. We have thus far attempted two different approaches. First, we used ultrafiltrate centrifugation after performing the TEV cleavage reaction to further concentrate the combined fractions and to convert the M2 from aqueous buffer to methanol. Using this approach, the S31C M2 precipitated and had to be discarded. However, we successfully re-attempted this approach with G34C M2 by slowing the centrifugation speed down from 4000 x g to 3200 x g, which allowed us to keep the protein concentration low enough to avoid protein precipitation. We then reconstituted 0.05 mg of

G34C M2 (0.14 mg/ml) into 10 mg of lipid (POPC, POPG, and cholesterol at molar proportions of 3:1:2) and tested for functionality, as described in Sharma et al (6). Unfortunately, the M2 liposome samples did not differ from the M2-free controls in proton conductivity (i.e. the protein was not detectably functional), even though the full length G34C mutant of M2 is functional when expressed in oocytes (7). Presumably there was a problem with the tetramerization during the reconstitution.

In the second approach to reconstituting M2 into liposomes, we stopped the TEV cleavage reaction using trichloroacetic acid (TCA). The addition of TCA to the cleavage reaction resulted in precipitation of all proteins present. The precipitate was then collected using slow centrifugation and the resulting pellet was dried in a vacuum for 2.5 hours. The dried pellet was then gently stirred in 5 ml of methanol for 4.5 hours, after which the solution was centrifuged at 13,000 x g for 20 minutes and the supernatant was carefully collected. The approximate concentration of the M2 in methanol was obtained using a spectrophotometer. However, the tryptophan and peptide bond spectra seemed to be absent because the spectra lacked separate peaks at 220 nm and 280 nm.

In addition to our efforts of growing, harvesting, and purifying the M2 mutants, we have also made significant progress towards the synthesis of rimantadine thiol. We propose to synthesize rimantadine thiol (compound 6) using the schematic represented in Scheme 1. We have been successful in obtaining the epoxide intermediate (compound 3) in high yield (90%) and in performing the epoxide opening to obtain the azido alcohol (compound 4) with 82% yield. We have successfully synthesized aziridine (compound 5); however, purification of the aziridine product has been complicated by the large amount of PPh_3 in the product. Nevertheless, we have used the impure aziridine to yield rimantadine thiol, but in very low yield (5 mg).

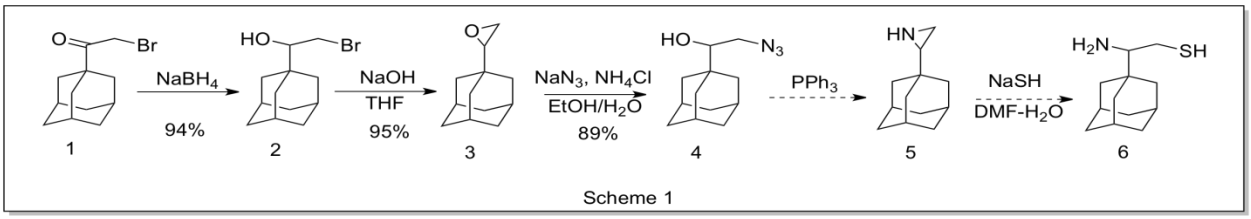

Scheme 1

Recommendations

Protein yield in our initial attempts was low (0.13 mg/ml ± 0.005); however, we were able to almost triple the yield of purified M2 (0.38 mg/ml ± 0.014) by adjusting our approach in several ways. First, we increased the incubation period when growing *E.Coli* from 37 hours to 49 total hours of incubation. Second, we decreased the incubation period of M2 with nickel column resin from 18 hours to 4 hours, an adjustment we made in order to reduce non-specific binding of M2 to the nickel resin. Third, we increased the volume of nickel resin from 0.5 ml to 1.0 ml in order to avoid saturation of the nickel resin. Fourth, we improved nickel column elution techniques (e.g. using the same volume of elution buffer as there was nickel resin, adding the elution buffer to the resin drop wise, and ensuring that the nickel resin was level when eluting the column).

When performing TEV cleavage, it appeared that more protease was required to carry out the reaction when the MBP-M2 construct was still bound to the column resin than when the MBP-M2 construct was eluted from the column before carrying out the TEV protease reaction. Because the protease has an HQ (His-) tag that binds to nickel resin with high affinity, a higher volume of nickel resin may be required when carrying out the TEV protease reaction with the MBP-M2 construct still bound to the column resin in order to avoid saturation of the resin by the TEV protease, and/or that the TEV protease may be inactivatined (isolated) by binding to resin. Therefore, eluting the column before carrying out the TEV protease reaction was our preferred

approach because it appeared to require less protease and the protease is probably better able to catalyze the reaction because it is not being sequestered by the nickel resin.

As described in the Report section above, Figure 2 shows a Tris-Hepes-SDS gel of purified MBP-M2 (again, the 22-62 truncate with the S31C mutation). We expected the lanes containing MBP-M2 (lanes 4, 6-10) to display a prominent, clean band at approximately 49 kD. The smeared appearance of lane 1 (containing post-lysis supernatant) confirms that an array of proteins was present in the sample following bacterial lysis as expected. The clean appearance of lane 3 confirms that all of the proteins not bound to the nickel resin with high affinity were successfully washed out of the column by the initial column wash with 25 mM imidazole. Lane 3 also serves as a negative control, confirming that the bands present in lane 4 and lanes 6-10 are not artifacts resulting from photography of the gel. The protein ladder (Invitrogen, Carlsbad, CA) in lane 5 serves as a positive control, suggesting that the gel was run correctly. We are puzzled by the presence of the bands at 10 kD, 15 kD, 25 kD, and 60 kD.

In order to increase our confidence in running Tris-Hepes-SDS gels, we ran a series of gels using maltose binding protein, BSA, and β-lactogolublin as protein standards. We prepared approximately 50 μg of each protein standard using the sample preparation procedures described above in *Methods*. The resulting bands from these protein standards did correspond roughly (± 10 kD) to their known molecular weights; however, the bands were somewhat smeared on the gel and were rounded in appearance, perhaps due to gel overloading. Before running our most recent protein standard gel, we prepared new gel running buffer. The new running buffer did not improve the gel results. **We recommend further investigating trouble-shooting procedures for running Tris-Hepes-SDS gels.**

Figure 3 shows a Tris-Hepes-SDS gel of post-cleavage column-eluted MBP and TEV protease (lane 1), post-cleavage M2 (22-62)S31C (lane 3), and pre-cleavage MBP-M2 (lanes 4-7). As in figure 2, the smeared appearance of the lane containing the post-lysis unpurified supernatant (lane 10) confirms that an array of proteins was present in the sample following bacterial lysis. The clean appearance of the column wash in lane 8 confirms that all of the proteins not bound to the nickel resin with high affinity were successfully washed out of the column. The protein ladder (Thermo Fisher Scientific Inc., Rockford, IL) in lane 9 serves as a positive control, suggesting that the gel was run correctly. We are puzzled by the many fine bands present in this gel. The absence of bands in the empty lane (lane 2) confirms that these fine bands, as well as the bands in lanes 4-7, are not artifacts resulting from photography of the gel. **In addition to further investigating trouble-shooting procedures for running Tris-Hepes-SDS gels, we also recommend further investigation of trouble-shooting procedures for protein purification using affinity chromatography.**

We preferred using the TCA/methanol method of M2 purification rather than the nickel column/ultrafiltrate centrifugation method of purification. This works, as we understand from Dr. Sharma, because only M2 dissolves in the MeOH. We feel that less sample is lost when using the methanol purification approach than when running the sample through an additional nickel column. Presumably, less M2 was recovered when using the ultrafiltrate centrifugation method than when using the TCA/methanol method due to M2 adherence to the filter device, possible damage to the filter device because of its incompatibility with pure methanol, and a higher risk of irreversible M2 precipitation when using ultrafiltrate centrifugation.

We have made progress towards successfully growing, harvesting, and purifying M2 mutants; however, successful synthesis of rimantadine thiol is of equal importance to the

completion of this project. During synthesis of rimantadine thiol (scheme 1, compound 6), we performed the epoxide opening to obtain the azido alcohol (compound 4). Initially, the reaction rate was quite slow, resulting in low yield of the azido alcohol. However, by increasing the reaction time from 3 hours to approximately 15 hours, and by increasing the amount of NH_4Cl from 1 molar equivalent to 2 molar equivalents, we were able to obtain the azido alcohol intermediate with 82% yield. Purification of aziridine (compound 5) has been difficult due to the large amount of PPh_3 in the product. In order to reduce the amount of PPh_3 contamination, we are currently attempting the aziridine formation reaction using less PPh_3 (1.1 molar equivalents instead of 1.5 molar equivalents). We are confident that purifying the aziridine intermediate will allow us to achieve a greater yield of the rimantadine thiol product.

Acknowledgments

This research was supported by an ORCA Student Fellowship grant from Brigham Young University's Office of Research and Creative Activities and by an Undergraduate Research Award from Brigham Young University's Department of Chemistry and Biochemistry. We gratefully acknowledge Ian Nelson for performing the site-directed mutagenesis and bacterial transformation as well as Dr. David Busath and Dr. Steven Castle for their supervision and support throughout this project.

References

1. Schnell JR, Chou JJ. Structure and mechanism of the M2 proton channel of influenza A virus. Nature 2008;451:591.
2. Stouffer AL, Acharya R, Salom D, Levine AS, Di Costanzo L, Soto CS, Tereshko V, Nanda V, Stayrook S, DeGrado WF. Structural basis for the function and inhibition of an influenza virus proton channel. Nature 2008;451:596-599.
3. Cady SD, Schmidt-Rohr K, Wang J, Soto CS, DeGrado WF, Hong M. Structure of the amantadine binding site of influenza M2 proton channels in lipid bilayers. Nature 2010;463:689.
4. Dawson PE, Muir TW, Clark-Lewis I, Kent SB. Synthesis of proteins by native chemical ligation. Science 1994;266(5186):776.
5. Zhan C, Varney KM, Yuan W, Zhao L, Lu W. Interrogation of MDM2 phosphorylation in p53 activation using native chemical ligation: The functional role of Ser17 phosphorylation in MDM2 reexamined. JACS 2012, epub.
6. Sharma M, Yi M, Dong H, Qin H, Peterson E, Busath DD, Zhou H, Cross TA. Insight into the mechanism of the influenza A proton channel from a structure in a lipid bilayer. Science 2010;330:509.
7. Shuck K, Lamb RA, Pinto, LH. Analysis of the pore structure of the influenza A virus M2 ion channel by the substituted-cysteine accessibility method. J Virol 2000;74:7755-7761.

Figure Legends

Figure 1: The principle of native chemical ligation. The synthetic segment, peptide 1, which contains a thioester at the α-carboxyl group, undergoes nucleophilic attack by the side chain of the Cys residue at the amino terminal of peptide 2 (R is an alkyl group). The initial thioester ligation product undergoes rapid intramolecular reaction because of the favorable geometric arrangement [involving a five-membered ring] of the α-amino group of peptide 2, to yield a product with a native peptide bond at the ligation site. Both reacting peptide segments are in completely unprotected form, and the target peptide is obtained in final form without further manipulation (4).

Figure 2: Tris-Hepes-SDS gel of M2-MBP (S31C). Lane 1 contains supernatant collected following bacterial lysis and centrifugation. Lane 2 contains supernatant collected following sample incubation with octyl glucoside and centrifugation. Lane 3 contains Ni column wash collected following supernatant run-through of the column. Approximately the last 0.5 ml were collected of the 10 ml of 25 mM imidazole wash buffer used. Lanes 4, 6-10 contain column elution fractions (fraction 1 is the first fraction collected using 250 mM imidazole, followed by fraction 2, etc.). Lane 5 contains the protein ladder (Invitrogen, catalog # LC5800).

Figure 3: Tris-Hepes-SDS gel of TEV-cleaved M2 (S31C), column-eluted MBP and TEV protease, and M2-MBP (S31C). (See below for relation of the reaction procedure to the lane assignments). Lane 1 contains the column elution (250 mM imidazole) after running the TEV cleavage reaction in a beaker, injecting the well-stirred products into the Ni column, and collecting the run-through. Lane 2 is an empty lane (negative control). Lane 3 contains the column run-through following the externally performed TEV cleavage reaction. Lanes 4-7 contain column elution fractions (fraction 1 is the first fraction collected, followed by fraction 2, etc.). Lane 8 contains column wash collected following supernatant run-through of the column (approximately the last 0.5 ml were collected of the 10 ml of wash buffer used). Lane 9 contains the protein ladder (Thermo Fisher Scientific Inc., product # 26619). Lane 10 contains supernatant collected following bacterial lysis and centrifugation.

Figure 1

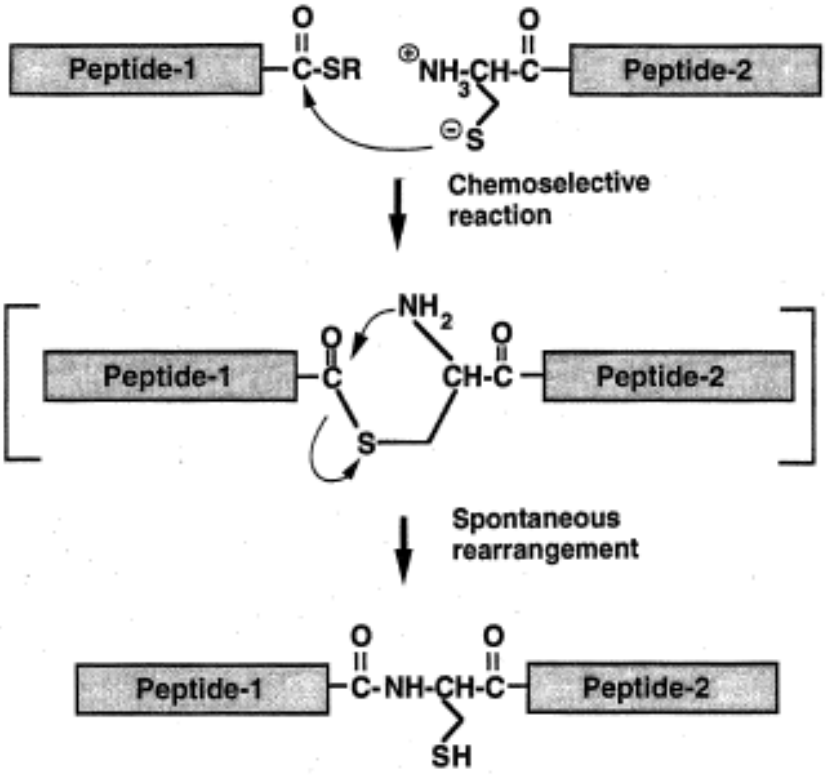
Peptide-1
C-SR
NH3CH-C
Peptide-2
S
Chemoselective reaction
NH2
Peptide-1
C
CH-C
Peptide-2
S
Spontaneous rearrangement
Peptide-1
C-NH-CH-C
Peptide-2
SH

Figure 2

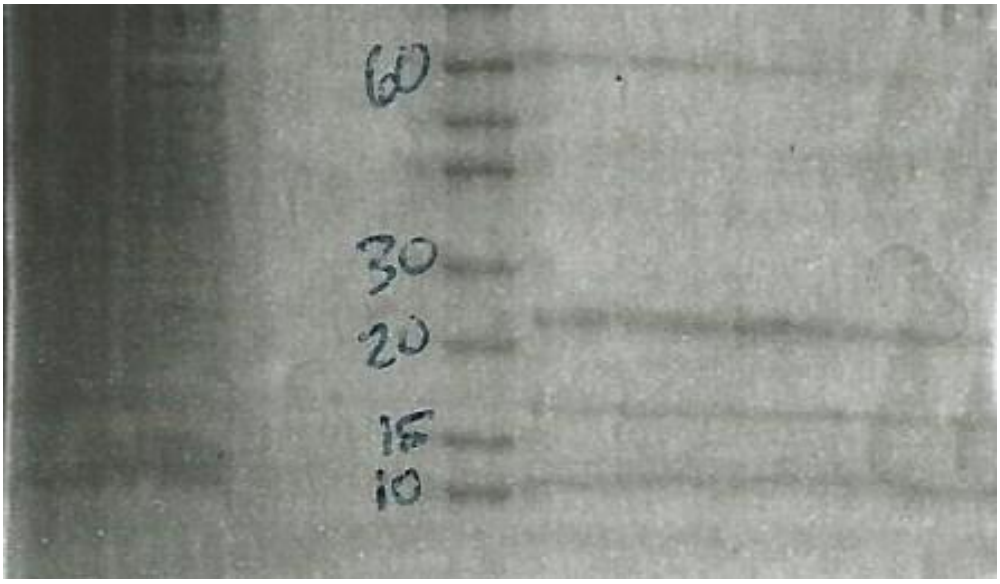
Post-lysis Supernatant
Post-incubation supernatant with O.G. Detergent
Column Wash
MBP-M2 (S31C) Fraction 1
Ladder
MBP-M2 (S31C) Fraction 2
MBP-M2 (S31C) Fraction 3
MBP-M2 (S31C) Fraction 4
MBP-M2 (S31C) Fraction 5
MBP-M2 (S31C) Fraction 6
60
30
20
15
10
1
2
3
4
5
6
7
8
9
10

Figure 3

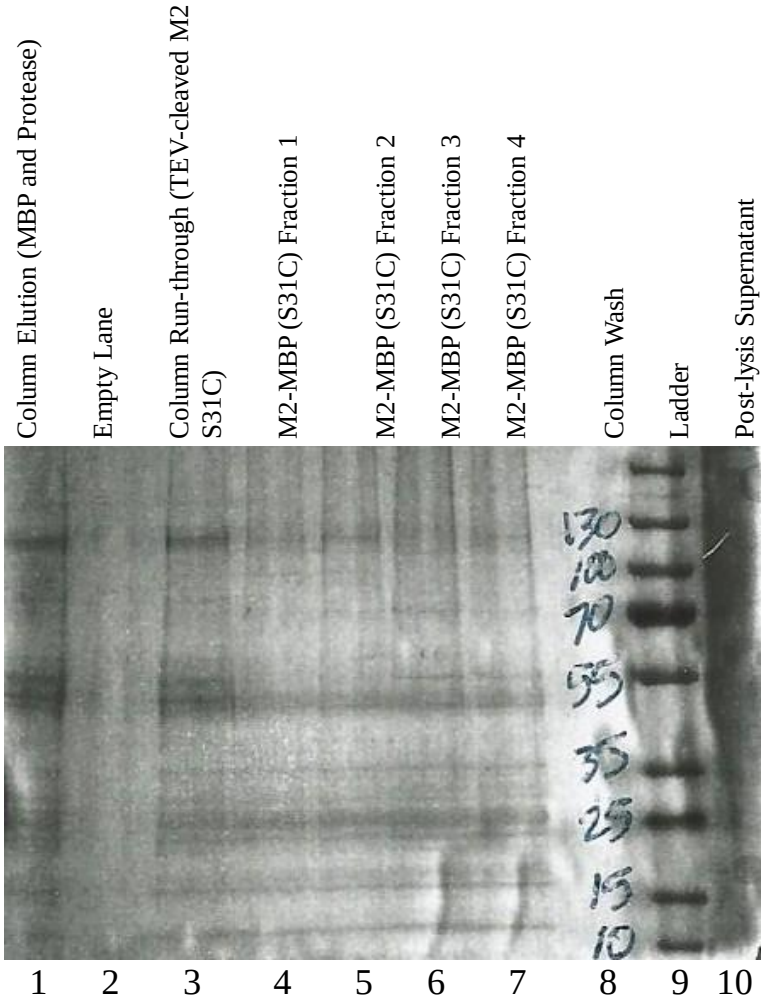
Column Elution (MBP and Protease)
Empty Lane
Column Run-through (TEV-cleaved M2 S31C)
M2-MBP (S31C) Fraction 1
M2-MBP (S31C) Fraction 2
M2-MBP (S31C) Fraction 3
M2-MBP (S31C) Fraction 4
Column Wash
Ladder
Post-lysis Supernatant
130
100
70
55
35
25
15
10
1 2 3 4 5 6 7 8 9 10